We choose the turbulent Prandtl expression of Jischa and Rieke,[5] which is

$$Prt = \epsilon_m/\epsilon_h = a + b(Pr+1)/Pr \tag{23}$$

with $a=0.825$ and $b=0.0309$, a result fitting data for air ($Pr=0.7$) quite well.

Results and Discussion

The numerical procedure of solving the boundary-layer equations and the heat conduction equation are identical to that in Ref. 1. The dimensionless overall rate of heat transfer Q from the pin can be expressed as

$$\frac{Q}{r_0 k(T_0-T_\infty)Re_L^{1/2}} = \frac{2\pi}{N_c}\left.\frac{d\theta_f}{d\xi}\right|_{\xi=1} \tag{24}$$

or

$$\frac{Q}{r_0 k(T_0-T_\infty)Re_L^{1/2}} = 2\pi\int_0^1 \left(-\frac{\partial\theta}{\partial\eta}\Big/\xi^{1/2}\right)_{\eta=0} d\xi \tag{25}$$

The overall heat-transfer rate of the pin in the pure laminar flow and the mixed laminar and turbulent flow are shown in Fig. 1. It is observed from Fig. 1 that an increase in N_c yields a decrease in the corresponding overall heat transfer rate. Figure 1 also shows that the overall heat-transfer rate of the pin in the turbulent flow is higher than that of the pin in the laminar flow. This behavior is due to the action of turbulent eddies that increases the local heat transfer rate at the wall.

Figure 2 illustrates the local heat-transfer coefficient along the pin surface for various values of N_c. The local heat-transfer coefficients can be written in dimensionless form as

$$\frac{hL}{kRe_L^{1/2}} = -\frac{\theta'(\xi,0)}{\theta_f \xi^{1/2}} \tag{26}$$

As seen from Fig. 2, the distribution of the local heat-transfer coefficient $\hat{h}$ decreases monotonically before the transition zone along the streamwise direction, but the $\hat{h}$ becomes irregular in the transition zone due to the occurrence of the random spots of turbulence. This figure also shows that the larger values of N_c give rise to larger values of $\hat{h}$. It is observed from Fig. 2 that the turbulent-affected local heat-transfer coefficient is higher than $\hat{h}$ of the pin surface in pure laminar flow.

Figure 3 presents pin temperature distributions in turbulent forced convective flow. The figure illustrates that the larger values of N_c give rise to larger variations of pin temperature distributions. The phenomenon of this behavior is the same as the forced convective laminar flow over a circular pin.[1] Figure 3 also shows the the temperature distributions of the pin in the turbulent flow give a larger variation than those of the pin the laminar flow ($\epsilon_m/\epsilon_h=0$). This behavior is attributed to enhanced surface heat-transfer rate associated with an increase in the random spots of turbulence along the streamwise direction.

References

[1]Huang, M. J., Chen, C. K., "Vertical Circular Pin with Conjugated Forced Convection-Conduction Flow," *Journal of Heat Transfer, Transactions of ASME*, Vol. 106, 1984, pp. 658-661.

[2]Huang, M. J. and Chen, C. K., "Conjugated Mixed Convection and Conduction Heat Transfer Along a Vertical Circular Pin," *International Journal of Heat and Mass Transfer*, Vol. 28, No. 3, pp. 523-529, 1985.

[3]Lien, F. S., Chen, C. K., and Cleaver, J. W., "Vertical Plate Fin with Conjugated Forced Convection-Conduction Turbulent Flow," ASME Paper 84-WA/HT-8, 1984.

[4]Cebeci, T. and Smith, A.M.O., "Analysis of Turbulent Boundary Layers," Academic Press, New York, 1974.

[5]Müller, U., Rosener, K. G., and Schmidt, B., (eds.), *Recent Development in Theoretical and Experimental Fluid Mechanics*, Springer-Verlag, Berlin, 1979.

Pressure Fluctuations on Hypersonic Vehicles Due to Boundary-Layer Instabilities

A. Demetriades*
Montana State University, Bozeman, Montana

IT is generally agreed that a sequence of intense traveling waves appears in the hypersonic laminar boundary layer of cones in the region preceding the transition to turbulence.[1-7] Consisting of oscillations in the fluid velocity, density, and temperature, these waves are aligned with their fronts normal to the flow vector and are apparently due to the so-called second instability mode predicted by linear stability theory.[8] The connection of these "laminar waves," which represent the selective amplification of small ambient disturbances, to transition has been under experimental study for some time; their regularity and intensity, however, extends their possible importance beyond the issue of stability. For example, these waves may be dependable announcers of impending transition and may be ubiquitous and dominant features of the laminar portion of the flowfield, even for pitching or rolling (maneuvering) vehicles. Furthermore, because of the great strength of vorticity-generated pressure waves at hypersonic speeds, they may be important sound and vibration generators. These questions should be of interest to vehicle designers and are addressed in this Note.

Two recent experiments[9,10] performed in Tunnel B of the Arnold Engineering Development Center (AEDC) now provide interesting new results concerning the detection of the waves microphonically and also while the cone is pitching or rolling. Both tests were done in AEDC's Wind Tunnel B at stream Mach number $M_\infty=8$ (edge $M_e=7$) on slender, sharp-tipped cone models on which transition events were recorded over a wide variety of simulated "maneuvers"; these included both static and dynamic (continuous) changes in unit Reynolds number Re' and angle of attack α and also rolling motions at angle of attack. Attached flush on the surface of the models were a number of commercial pressure transducers acting as "surface microphones." Also installed within the structure of the models were a number of special "subsurface" pressure-sensitive transducers† separated from the airflow by a portion of the model structure skin that was 0.38 cm thick ATJ graphite in the first experiment[9] and carbon phenolic of thicknesses of 0.13-0.76 cm in the second.[10] This solid "shield" interposed over the subsurface microphones protected the latter from the hot fluid (and, in flight, from bombardment by ablation products); but it could also divert to the sensors acoustic signals from remote stations of the model through its structure and thus decrease their sensitivity to purely local events.

To test this possibility and to evaluate both the surface and the subsurface microphones as indicators of localized pressure fluctuations on the model, a variety of additional sensors were utilized for comparison. These consisted of the wind tunnel shadowgraph system, model surface pressure taps, surface thermocouples and heat-transfer (Gardon) gages, and externally supported probes such as pitot and pitot-acoustic (dynamic pitot) probes and hot-film anemometers. The surface and subsurface microphones and the film anemometer had a frequency response suitable for

Received Feb. 21, 1985.

*Professor, Department of Mechanical Engineering.

†Designated as "boundary-layer acoustic monitors" or BLAM by their manufacturer, Kaman Sciences Corporation, Colorado Springs, CO.

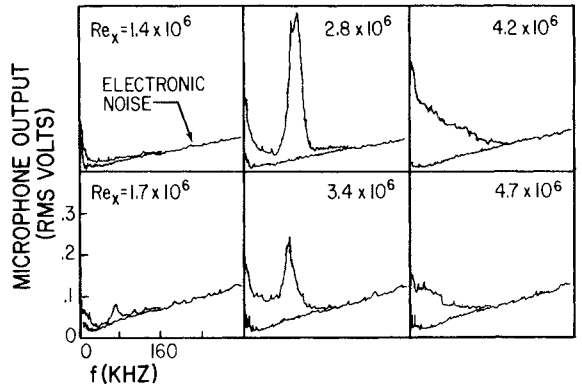

Fig. 1 Output spectra of surface microphones located on the same ray at 85 cm (top) and 103 cm (bottom) from the cone tip during a continuous variation of unit Reynolds number, at $\alpha = 0$ deg.

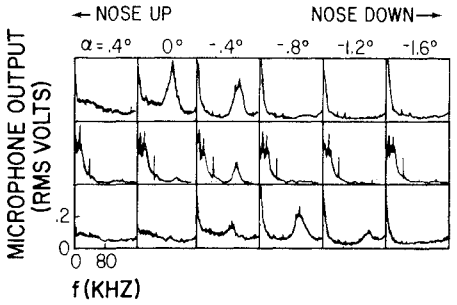

Fig. 2 Output spectra of the surface microphones at 85 cm (top row) and 103 cm (bottom row) from the tip and of a subsurface microphone (middle row) at 85 cm during a continuous pitching-down maneuver at a unit Reynolds number of 10^6/ft.

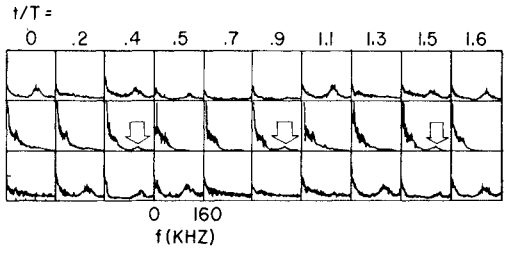

Fig. 3 Ouput spectra, at various intervals of the roll period T, of the surface microphones at 85 cm (top row) and 103 cm (bottom row) and of the subsurface microphone at 85 cm (middle row) during model roll at $\alpha = 1.25$ deg and $Re' = 10^6$/ft.

responding to the cone boundary-layer turbulence and far exceeding the frequencies inherent in the model maneuvers. Special attention was paid to spurious noise in the microphones due to the electronics, to structural vibrations, and even to sound radiation from the wind tunnel sidewalls. For example, a special test was made to see if microphone outputs, mistaken for boundary-layer signals, could be generated by water circulating in various cooling conduits within the model. As another example, the direct tunnel sidewall radiation effect on the microphones was checked by asymmetrically tripping the model boundary layer with a roughness patch. As a result of such tests, which are detailed in Ref. 9, the influence of extraneous factors on the data presented here was identified and minimized or eliminated.

The consensus of the nonmicrophonic sensors employed in these two experiments showed an orderly and repeatable transition process on the cone models. For example, at $\alpha = 0$ deg, transition began at a wetted-length Reynolds number $Re_x \simeq 4 \times 10^6$. Nearly identical results have been routinely obtained in the same wind tunnel with similar slender cone models over the past several years.[2,6,11] Hot-wire and hot-film anemometers immersed in the boundary layer on such occasions, past and present, have regularly detected the amplified laminar waves; typically, the waves become visible as early as $Re_x = 10^6$ with frequencies of 50-200 kHz and have a wavelength very nearly twice[5,6] the boundary-layer thickness δ. Their detection has been so far limited to the flow-immersible sensors mentioned and to the wind tunnel optics. We shall now show evidence that they also create intense pressure fluctuations detected by the surface and subsurface microphones.

Figure 1 shows the output spectrum of two surface microphones, one at 85 cm and the other at 103 cm from the cone tip, obtained at $\alpha = 0$ deg as the wind tunnel pressure was varied over the range $0.5 < Re' < 2 \times 10^6$/ft. Apparently, the laminar waves cannot be sensed for $Re_x < 1.5 \times 10^6$, but they are thereafter clearly seen at about 100 kHz and, of course, vanish after turbulence has been established at about $Re_x = 4 \times 10^6$. The observed frequency is in full agreement with the $f \doteq U_e/2\delta$ rule noted earlier (U_e is the edge velocity); in fact, if plotted in the nondimensional coordinates of stability diagrams (e.g., Fig. 8 of Ref. 5), the energy peaks of Fig. 1 would produce points on the upper neutral branch of the second unstable mode. The outstanding feature of this wave motion, however, is its intensity: the contribution of this motion is seen, from the spectra of Fig. 1, to equal or exceed all those at other frequencies, whether in laminar or turbulent flow.

A demonstration of a typical subsurface microphone response is combined in Fig. 2 with a view of a continuous pitching (angle of attack) maneuver at $Re' = 10^6$/ft as recorded by such a sensor. This figure shows the response of the two surface microphones of Fig. 1 (top and bottom row) and of a subsurface microphone at 85 cm from the tip (middle row) at a depth of 0.76 cm during continuous "pitching-down" motion (from $\alpha > 0$ to < 0 deg). All three sensors were located along the top ray of the cone and the graphs in each row show the output spectra at the indicated angles of attack. When $\alpha > 0$ deg, all three sensors are on the leeward meridian ray and, when $\alpha < 0$ deg, they are on the windward meridian ray; the spectra for $\alpha > 0$ deg on the left side of Fig. 2 indicate turbulent flow and those on the right for $\alpha < 0$ deg show laminar flow for all three sensors, indicative of the well-known transition asymmetry for pitched cones (e.g., see Fig. 2 of Ref. 12).

The transition between these two regions is again marked by spectrum peaks at the laminar wave frequency. The emphasis here is on the complete coincidence in the peak frequencies between the subsurface and surface microphones lying at the same position on the model (which are represented by the first two rows of Fig. 2). Note that the subsurface microphone signal at the laminar wave frequency is a smaller part of its total output, which also includes intense low-frequency signals due to incoherent electronic and structural noise. Another example of microphonic response to the laminar waves is shown on Fig. 3. Here, the model is rolling with period $T = 1$ rev/s at $Re' = 10^6$/ft while pitched at $\alpha = 1.25$ deg and the spectra of two surface microphones (first and third row) and the subsurface microphone (second row) are recorded at intervals of $T/6$. The two surface microphones detect the laminar waves at different times in the roll cycle because of their displacement along the same cone ray and because of the asymmetric transition on the yawed model. The subsurface sensor, located at the same spot as the top surface microphone, detects the laminar waves, albeit faintly (arrows on Fig. 3) in coincidence with the latter.

Predictably, all subsurface microphone response to the laminar waves usually deteriorated as the distance between the surface and the transducer increased, i.e., when the

microphone was buried deeper within the surface. It would serve no useful purpose to further trace this attenuation in the interior model structure at this point, which is complex and peculiar to the model design.

This work has demonstrated that flow instabilities at hypersonic speeds generate intense pressure fluctuations on the cone surface, which do penetrate the surface to some distance and which persist with regularity even when the cone executes maneuvers relative to the flight vector such as pitch and roll. At a boundary-layer edge Mach number M_e of about 7, the results of Refs. 2, 4, 5, etc., indicate that the frequency of these oscillations scales with f and the edge velocity U_e as $f \doteq U_e/2\delta$; it should be noted,[13] however, that this scaling is invalid for $M_e < 2.5$. Finally, it must be also noted that these are Mach number ranges (e.g., $M_e \simeq 3$) for which monochromatic oscillations do not appear[3,14] and that at still lower M_e levels the laminar waves would be incapable of producing pressure fluctuations intense enough to be detected on the surface.

Acknowledgment

This work was supported by U.S. Air Force Contracts F04701-77-C-0113 and F04701-72C-0027.

References

[1]Potter, J. L. and Whitfield, J. D., "Boundary-Layer Transition Under Hypersonic Conditions," AGARDograph 97, Pt. III, May 1965.

[2]Demetriades, A., "Hypersonic Viscous Flow Over a Slender Cone, Part III: Laminar Instability and Transition," AIAA Paper 74-535, June 1974.

[3]Kendall, J. M. Jr., "Wind-Tunnel Experiments Relating to Supersonic and Hypersonic Boundary Layer Transition," *AIAA Journal*, Vol. 13, March 1975, pp. 290-299.

[4]Demetriades, A., "Boundary Layer Stability Observations at Mach No. 7," *Transactions of ASME, Journal of Applied Mechanics*, Vol. 99, Jan. 1977, pp. 7-10.

[5]Demetriades, A., "New Experiments on Hypersonic Boundary Layer Stability Including Wall Temperature Effects," *Proceedings of the 1978 Heat Transfer and Fluid Mechanics Institute*, Stanford University Press, Stanford, CA, 1978, pp. 39-55.

[6]Stetson, K. F., Thompson, E. R., Donaldson, J. C., and Siler, L. G., "Laminar Boundary Layer Stability Experiments on a Cone at Mach 8, Part 1: Sharp Cone," AIAA Paper 83-1761, July 1983.

[7]Stetson, K. F., Thompson, E. R., Donaldson, J. C., and Siler, L. G., "Laminar Boundary Layer Stability Experiments on a Cone at Mach 8, Part 2: Blunt Cone," AIAA Paper 84-0006, Jan. 1984.

[8]Mack, L. M., "Linear Stability Theory and the Problem of Supersonic Boundary-Layer Transition," *AIAA Journal*, Vol. 13, March 1975, pp. 278-289.

[9]Demetriades, A. and Laderman, A. J., "Hypersonic Boundary Layer Transition as Detected with a Submerged Acoustic Sensor," Final Report, Boundary Layer Acoustics and Transition Program, Ford Aerospace and Communications Corp., Newport Beach, CA, March 1979.

[10]Nickell, J. C. and Demetriades, A., "Evaluation of Boundary Layer Transition Sensors in a Hypersonic Wind-Tunnel Environment," Paper presented at 27th International Instrumentation Symposium, Instrument Society of America, April 1981.

[11]Martellucci, A. and Laganelli, A., "Hypersonic Viscous Flow over a Slender Cone, Part I: Effect of Reynolds Number, Blowing and Angle of Attack on Viscous Layer Properties," AIAA Paper 74-533, June 1974.

[12]Stetson, F. K., Thompson, E. R., Donaldson, J. C., and Siler, L. G., "Laminar Boundary Layer Stability Experiments on a Cone at Mach 8, Part 3: Sharp Cone at Angle of Attack," AIAA Paper 85-0492, Jan. 1985.

[13]Laufer, J. and Vrebalovich, T., "Stability and Transition of a Supersonic Laminar Boundary Layer on an Insulated Flow Plate," *Journal of Fluid Mechanics*, Vol. 9, No. 2, 1960, pp. 257-299.

[14]Demetriades, A., "Supersonic Boundary Layer Stability over a Rough Wall," Final Report, AFOSR Grant 80-0267, Jan. 1985.

Effects of Electric Fields on the Flame Propagation Velocity of Methane-Air Flame

R.I. Noorani*
The University of Southwestern Louisiana
Lafayette, Louisiana
and
R.E. Holmes†
Texas A&M University, College Station, Texas

Introduction

THIS Note presents the experimental results of the effects of longitudinal and transverse electric fields on the flame propagation velocity of premixed methane-air flame in a vertical tube. This is the second and final report of an earlier investigation[1] in which the effects of electric fields on blowoff limits of methane-air flame were reported.

Observations of changes in flame geometry and propagation velocities under the influence of electric fields have been made for many years. Evidence indicating an increase in flame propagation velocity is incomplete and contradictory.[2-5] Under similar conditions, electric fields are known to have increased, slowed down, or extinguished combustion. The position effects of electric fields on blowoff limits of methane-air flame have encouraged the authors to undertake the present investigation.

Apparatus and Procedures

The experimental configuration for the determination of flame propagation velocity of methane-air flame is shown in Fig. 1. The experiment was conducted at room temperature (76 deg) and atmospheric pressure (760 mm Hg).

The experimental apparatus consists of a vertical pyrex glass tube (151 cm long, 5 cm i.d.), a polyethylene mixing pump, platinum electrodes, capillary tubes, a mercury reservoir, photodiodes, and other components, as shown in Fig. 1. A manometer was used to indicate the amount of evacuation of the vertical flame tube and to make sure that no undetected leaks developed in the system.

Two TIL-63-type photodiodes were used to detect light signals from propagating flames. A longitudinal electric field was obtained by placing two aluminum rings (1.54 cm wide and 5 cm in diameter) around the glass tube, 5 cm apart. The upper ring was then connected to the positive terminal of the high-voltage supply. A transverse electric field was established between two 110-cm-long, 2.54-cm-wide segments of aluminum pipe placed diametrically opposed to each other outside the pyrex tube and held by masking tape. The two electrodes so formed were connected to the positive and ground terminals of the high-voltage supply.

Before an experiment, the barometer and manometer readings were taken. The gas and air, dried by passing through a drying tube containing calcium chlorides, were then admitted into the flame tube. The mixture composition was measured accurately by admitting the components slowly through the needle valves and measuring the partial pressures with the mercury manometer.

The mixing of gas and air was done by the mixing pump which was operated for about 15-20 min for stoichiometric mixtures and 25-30 min for rich or lean limit mixtures.

Received Jan. 18, 1985; revision received June 19, 1985.

*Assistant Professor, Department of Mechanical Engineering.
†Associate Professor, Department of Mechanical Engineering.